Uncertainty in Parameterized Convection Remains a Key Obstacle for Estimating Surface Fluxes of Carbon Dioxide

Andrew E. Schuh[1] and Andrew R. Jacobson[2,3]

[1]Cooperative Institute for Research in the Atmosphere (CIRA), Colorado State University, Fort Collins, CO USA
[2]CIRES, University of Colorado, Boulder, CO USA
[3]NOAA Global Monitoring Laboratory, Boulder, CO USA

Correspondence: Andrew Schuh, aschuh@atmos.colostate.edu

Abstract. The analysis of observed atmospheric trace gas mole fractions to infer surface sources and sinks of chemical species relies heavily on simulated atmospheric transport. The chemical transport models (CTMs) used in flux inversion models are commonly configured to reproduce the atmospheric transport of a general circulation model (GCM) as closely as possible. CTMs generally have the dual advantages of computational efficiency and improved tracer conservation compared to their parent GCMs, but they usually simplify the representations of important processes. This is especially the case for high-frequency vertical motions associated with diffusion and convection. Using common-flux experiments, we quantify the importance of parameterized vertical processes for explaining systematic differences in tracer transport between two commonly-used CTMs. We find that differences in modeled column average CO_2 are strongly correlated with the differences in the models' convection. The parameterization of diffusion is more important near the surface due to its role in representing PBL mixing. Accordingly, simulated near-surface *in situ* measurements are more strongly impacted by this process than are simulated total-column averages. Both diffusive and convective vertical mixing tend to ventilate the lower atmosphere, so near-surface measurements may only constrain the net vertical mixing and not the balance between these two processes. Remote sensing-based retrievals of total column CO_2, with their increased sensitivity to convection, may provide important new constraints on parameterized vertical motions.

1 Introduction

The analysis of atmospheric CO_2 mole fraction observations, including both *in situ* measurements and remote sensing retrievals of column average CO_2 (XCO2), depends heavily on knowledge of atmospheric transport. This is the case for flux inversion models which use simulated atmospheric transport to interpret measured gradients of trace gas mole fractions to estimate surface fluxes of those species. Determining the magnitude, distribution, and causes of terrestrial and oceanic carbon sinks by interpreting CO_2 measurements in the context of modeled transport has a long history (Keeling et al., 1989a, b; Denning et al., 1999; Gurney et al., 2002; Stephens et al., 2007). The recent work of Schuh et al. (2019) demonstrates that despite many years of progress in improving transport models, uncertainty and bias in simulated transport remains a key source of uncertainty in atmospheric inverse model results. In that work, the authors found a systematic dependence between optimized fluxes for large zonal regions and the corresponding transport model used in that system. That analysis found that in an ensemble of

25   state-of-the-art inversion models, the biggest systematic differences in optimized annual sources and sinks are in the latitudinal band from the equator to 45°N (Figure S1). The northern midlatitudes between 23° N and 67° N generate some of the biggest CO_2 signals in the atmosphere, due to the magnitude and seasonality of surface fluxes. Fossil fuel CO_2 emissions also are concentrated in this latitude band, with large emitters in North America, Europe, and Asia accounting for almost 80% of the 10 PgC/yr global fossil fuel emissions (Oda, 2018). The majority of the land and ocean net sink inferred from inversions is also

30   concentrated in this zonal band. As a 2015-2018 mean, the OCO-2 v9 MIP inversion ensemble finds that this region accounts for between 75% and 80% (between 3.55 - 3.7 PgC/yr of the 4.63 PgC/yr total of the global land and ocean carbon sink (Peiro et al., 2021), depending on the use of either in situ (IS) constraints or land nadir plus land glint (LNLG) data. The terrestrial component of this mean sink is characterized by intense seasonal and diurnal variability, the signals of which are exported both polewards and equatorwards by advective and convective processes, which themselves are seasonally variable (D'Arrigo et al.,

35   1987; Barnes et al., 2016). The tropical and high-latitudes signatures of midlatitude surface exchange depend strongly on the rate at which emissions signals are exported from the midlatitudes.

    Key carbon cycle questions are subject to the uncertainty in the midlatitude export rate, the rate at which carbon is transported out of the atmospheric column over the midlatitudes, as simulated by chemical transport models (CTMs). A recurring question about the global carbon cycle is whether the long-term terrestrial carbon sink should be attributed to the tropics or to the

40   midlatitudes (e.g. Schimel et al. (2014)). Terrestrial ecosystems around the world are all affected by changes in climate and atmospheric composition, but certain processes repeatedly emerge as potential explanations for increasing terrestrial sinks in tropical, mid-latitude and artic zones. For the northern midlatitudes, these theories include recovery from past land use practices and the impacts of nitrogen deposition (Norby and Zak, 2011; Craine et al., 2018; Penuelas et al., 2020). At higher latitudes, the expansion of boreal forests due to changing climate plays a role (Malhi et al., 1999), but the importance of that process is yet

45   to be fully established. In the tropics, an area dominated by high gross primary production year-round, uncertainties dominate our understanding of the relative impacts of deforestation, climate forcing, and CO_2 fertilization (Lloyd and Farquhar, 2008; Norby and Zak, 2011). Uncertainties for fluxes inferred from inversions in these large zonal bands are still too large to make confident statements about mean annual CO_2 fluxes, their annual cycles, and therefore, their causes. Another topic of current interest touched upon by the midlatitude export rate is the changing seasonal cycle amplitude (SCA) of atmospheric CO_2 mole

50   fractions at high latitudes (Graven et al., 2013; Liu et al., 2020). It is not clear the extent to which high-latitude carbon cycle processes are responsible for this observed growth in SCA, compared to the alternative possibility that this change is imported from midlatitudes.

    Research funded by both OCO-2 and ACT-America has established that the rate at which CO_2 flux signals are exported from the midlatitudes varies strongly between two of the most commonly used CTMs, GEOS-Chem and TM5 (Schuh et al., 2019).

55   This result was recently highlighted in Schuh et al. (2022) where the authors illustrated that the conclusions of a recent paper estimating the natural Chinese biospheric CO_2 sink (Wang et al., 2020) could be explained by differences among the CTMs being used in the atmospheric inversions considered.

    In this paper, we look into the causes for the differences in transport between GEOS-Chem and TM5 and show, in particular, that parameterized vertical mixing plays a key role in how inverse models built on these CTMs estimate surface sources

60 and sinks of CO_2. It is important to note that in order to simulate parameterized vertical mixing in CTMs, particularly deep convection, it is necessary to reduce the complexity, and often the time-space resolution, of the parent GCM model output. For example, an algorithm which iteratively recovers multiple subgrid scale plume structures such as the Relaxed Arakawa Schubert scheme must often be summarized in a CTM by a single plume structure often running at 5-10 times coarser time and space resolutions. Significant information could be lost in these averaging processes and could potentially impose meaningful

65 bias into estimates of vertical mixing. Even without such information loss, the GCMs producing some of the most commonly used reanalysis products in the world can differ dramatically in their estimates of convective activity. CTMs, particularly those used to advect long lived trace gases, must be able to simultaneously conserve tracer mass while attempting to faithfully reproduce transport from the GCM which produced the driving meteorology. This is particularly important when applied to convective mixing, as errors can often arise in parameterizations of this process, many of which were not designed with the

70 intent to move long lived tracers.

In summary, this work attempts to establish the degree to which transport differences between GEOS-Chem and TM5 are associated with parameterized convection and diffusion in the two models.

2 Methods

2.1 Transport Models

75 The simulations for TM5 and GEOS-Chem were run from the start of 2000 through the end of 2018 and the methodology closely follows what was performed in Schuh et al. (2019) with minor updates to transport model version and common CO_2 fluxes.

2.1.1 TM5/ERA-interim

TM5 is a global offline chemical transport model based on the predecessor model TM3 (Houweling et al., 1998; Dentener,

80 2003), with the capability of using two-way nested grids and including improvements in the advection scheme, vertical diffusion parameterization, and meteorological preprocessing of the wind fields (Krol et al., 2005). TM5 simulates advection, deep and shallow convection, and vertical diffusion in both the planetary boundary layer and free troposphere. For the analyses reported here, the model is driven by ECMWF ERA-interim (ERA-i) reanalysis meteorology, which is computed using a spectral formulation having 80 kilometers horizontal resolution. TM5 uses a 25 layer subset of ERA interim's 60 levels, extending to

85 0.01 hPa. Winds and mass fluxes from ERA-i are preprocessed by TM5 into coarse geographic grids, with attention to creating fields that conserve tracer and dry air mass. Like most numerical weather prediction models, advection in the parent ECMWF model is not strictly mass-conserving, so this preprocessing step is designed to enforce tracer mass conservation. This feature is considered crucial for long lived trace gas modeling. For simulations reported in this paper, TM5 was run at a global 3° longitude x 2° latitude resolution with a dynamically-variable time step with a maximum length of 90 minutes. This overall

90 timestep is dynamically reduced to maintain numerical stability, generally during times of high wind speeds. Transport opera-

tors in nested grids are modeled at shorter timesteps, so processes at the finest scales are conducted at an effective timestep of one-quarter the overall timestep. We will use "TM5" to refer to this configuration of TM5 with ERA-i meteorology.

Convective mass fluxes from ERA-i include entrainment and detrainment from both up- and down-drafts. These fluxes are combined into a convective mixing matrix representing mass transfer between cells within a vertical column. This mixing
95 matrix takes on the form of a tri-diagonal banded matrix with nonzero entries up to the cloud top, with nonzero non-diagonals allowing nonlocal mixing between all levels with convective activity within a single convective timestep. A description of this procedure in the TM3 model can be found in Heimann and Korner (2003). In TM5, vertical diffusive fluxes are then added to the convective mixing matrix and the summed mixing matrix is applied to the tracer mass vector for a column of air. In this scheme, convection and vertical diffusion are handled by a single step in the sequence of transport operators. To turn off
100 convection or diffusion in TM5, we interceded in this vertical mixing operator and nullified the mixing due to one or the other process.

2.1.2 GEOS-Chem/MERRA2

GEOS-Chem (Bey et al., 2001; Lin and Rood, 1996) is an offline global chemical transport model developed by an extensive global community of researchers, including teams at Harvard University and the Global Modeling and Assimilation Office
105 (GMAO) at NASA's Goddard Space Flight Center (GSFC). GEOS-Chem separately simulates advection, deep and shallow convection, and vertical diffusion in the planetary boundary layer. We use the version 12.0.2 of GEOS-Chem which has improved mass conservation (Lee and Weidner, 2016) and tracer advection over previous versions, but also includes modifications to more correctly simulate the impacts of variable water vapor content and dry air mass. Meteorology to drive the GEOS-Chem simulations is regridded from MERRA2 reanalyses (Rienecker et al., 2011; Bosilovich, 2015) to 2.5° longitude x 2° latitude.
110 GEOS-Chem is run using a 15 minute dynamical timestep. The native 72 levels of the MERRA2 grid are reduced to 47 levels for use in GEOS-Chem by aggregating levels above approximately 70hPa. This configuration of GEOS-Chem with MERRA2 meteorology is abbreviated "GEOS-Chem" in the following text.

Parameterized vertical motion in GEOS-Chem is composed of (1) moist convective processes and (2) planetary boundary layer (PBL) mixing. The Relaxed Arakawa–Schubert (RAS) scheme Moorthi and Suarez (1992) is used within the parent God-
115 dard Earth Observing System (GEOS) model used to create MERRA2. In particular, GEOS-5 uses an updraft-only detraining plume cloud model, which results in the two relevant output variables for GEOS-Chem convection: cloud upward moist convective mass flux and detrainment cloud mass flux. Convective transport in GEOS-Chem is then simulated with a single-plume scheme using the archived three hourly updraft and detrainment convective mass fluxes (Wu et al., 2007). It is worth noting that GEOS-Chem reproduces the three hourly average convective transport in the GEOS-5 GCM but any interaction of transport
120 and tracers on finer temporal scales is lost. Furthermore, whenever convection is found within a gridcell, the GEOS-Chem convection code triggers a complete mixing in the atmospheric column beneath the lowest level with convection. Because of this, diffusive mixing cannot be logically separated from convection in GEOS-Chem, especially in regions characterized by persistent convection.

The implementation of convective mixing in GEOS-Chem is intended to represent the single-updraft convection scheme
125 from its parent GEOS-5 model. The details of how this is done are described in Stanevich (2018). Among significant charac-
teristics are the use of a timestep, a sub-timestep of the GEOS-Chem transport timestep, specifically for convective processes,
and a sequential mixing algorithm. There is some question about the impacts of space- and time-averaging of parent-model
convective mass flux and vertical velocity fields on GEOS-Chem convection. These issues were explored by Yu et al. (2017),
who found that there are significant differences in GEOS-Chem transport as the resolution of the driving meteorology is varied.
130 Two options in GEOS-Chem exist for PBL mixing, (1) a non-local scheme based upon Holtslag and Boville (1993) adapted
for GEOS-Chem by Lin and McElroy (2010), and (2) a simple "well mixed" scheme in which PBL tracers are mixed evenly
from the surface to the top of the PBL as diagnosed by GEOS. In this work, we use the "well mixed" scheme in the PBL. Both
the convection and PBL mixing can be turned on or off using standard configuration options.

2.2 CO_2 simulations

135 We conduct CO_2 forward runs in both models from January 1, 2000 through December 31, 2018, similar to those in Schuh
et al. (2019) but with updated CarbonTracker fluxes. Initial CO_2 concentrations and surface fluxes throughout the simulation
come from the CarbonTracker CT2017 release (Peters et al., 2007, with updates documented at http://carbontracker.noaa.gov)
for the period January 1, 2000 to December 31, 2016 and then CT-NRT.v2019-2 for January 1, 2017 to December 31, 2018.
The initial condition field used by both models at January 1, 2000 was created by averaging together 15 years of CO_2 mole
140 fraction fields from CT2016, each sampled on January 1st of the years 2001-2015 and then scaled to the year 2000. The scaling
was performed by sampling the marine boundary layer from these mole fraction fields and then comparing them to the NOAA
marine boundary layer reference surface (https://www.gml.noaa.gov/ccgg/mbl) for the target date. For use in GEOS-Chem, the
CarbonTracker initial condition was interpolated vertically in pressure and horizontally in space to the GEOS-Chem grid as
described in Schuh et al. (2019).

145 CT2017 and CT-NRT.v2019-2 CO_2 optimized fluxes are partitioned into four flux terms: the imposed fossil fuel term, the
optimized biological flux, the imposed fire emissions flux, and the optimized oceanic flux. Each of these terms is tracked inde-
pendently as a tagged tracer, along with a background tracer representing the initial condition. As a result of the optimization
procedure, these fluxes are generally consistent with observed atmospheric CO_2 mole fractions. They were created with an
inverse modeling system based on TM5 and may have artifacts and inaccuracies associated with that model's atmospheric
150 transport and with assumptions used in the CarbonTracker data assimilation system. However, in the analyses conducted here
we do not require that these fluxes be completely correct, only that they are reasonably representative of actual atmospheric
CO_2 exchange with the surface. While there is certainly large uncertainty in CT2017 fluxes, important aspects of the flux
signals, such as seasonal terrestrial net ecosystem exchange in northern latitudes, placement of fossil fuel emissions, and esti-
mates of biomass burning are generally consistent with the results from other inversion systems that assimilate surface in situ
155 CO_2 data (Peylin et al., 2013). We found a small non-conservation of tracer mass in GEOS-Chem, with a loss of about 0.25%
in fossil fuel CO_2 over the period 2000-2018. Non-conservation of natural fluxes was about half as small. The global mass
differences for these tracers was removed from the 2016-2018 concentration data before analysis.

2.3 Vertical Mixing Perturbation Simulations

We ran three perturbation experiments on each transport model, with each simulation extending from Jan 1, 2016 to Dec 31,
160 2018. Control runs use the standard vertical transport in the models, unmodified from their stock configurations. The first
experiment involved turning off convection in both CTMs. These will be called the "no convection" or "NC" runs. The second
experiment involved leaving convection on but turning off diffusive mixing in the models. These will be termed "no diffusion"
("ND") runs. It should be noted that vertical advection as part of the resolved wind fields in each model still remains in both
perturbation and control runs for both models. We introduce the notion of a "convective effect", which we are defining as
165 control - NC and a "diffusive effect" as control - ND. The diffusive and convective transport effects are not independent.
The two processes have significant interactions such that total parameterized vertical transport is greater than the sum of the
convective and diffusive effects. Exploring this nonlinear interaction, while intriguing, is beyond the scope of this paper. As a
result, experiments in which both convection and diffusion are turned off will not be discussed.

3 Results

170 In this section, we show the differences between the TM5 and GC control simulations, and differences in the NC and ND cases
from several perspectives. First, we show a zonally averaged vertical "curtain" by latitude which illustrates how the differences
manifest themselves in the vertical. We then show two projections of the differences relevant to the major types of observational
data used in flux inversions of CO_2. The first is time-latitude (Hovmoller) plots of zonal-mean column-average CO_2 (XCO_2),
which is relevant to analysis of satellite CO_2 retrievals. The second is seasonal maps of differences in the planetary boundary
175 layer at 400 meters above ground level, meant to represent transport impacts on the ground-based *in situ* observational network.

3.1 Vertical curtains

Zonal average "curtains" (latitude by vertical dimension) of CO_2 from the control and NC simulations in the two models are
in presented in Figure 1. These curtains are shown for typical northern-hemisphere winter (February) and summer (August)
conditions. The expected buildup of CO_2 from fossil emissions and terrestrial biospheric respiration in boreal winter is evident
180 in the northern mid to high latitudes in both models' control simulations (panels a and b). The overall differences between
the GEOS-Chem and TM5 control runs are shown in panel (c). The convective effects in the two models for February, and
the GEOS-Chem minus TM5 difference in convective effect, are portrayed in the second row, panels d-f. The difference in
convective effects (panel f and l) bears a remarkable similarity to the control simulation difference (panel c and i).This suggests
visually that the GEOS-Chem minus TM5 difference in zonal-mean CO_2 is strongly driven by the convective effect. Indeed the
185 fields in are strongly correlated (February: panels a and c, r=0.72, p < 0.0001; August: panels d and f, r=0.83, p < 0.0001). This
will be further discussed in section 4 below. The diffusive effect (not shown here) is about three times larger in magnitude, but
is strongly concentrated near the surface. The diffusive effects are shown in Figures S2 and S3.
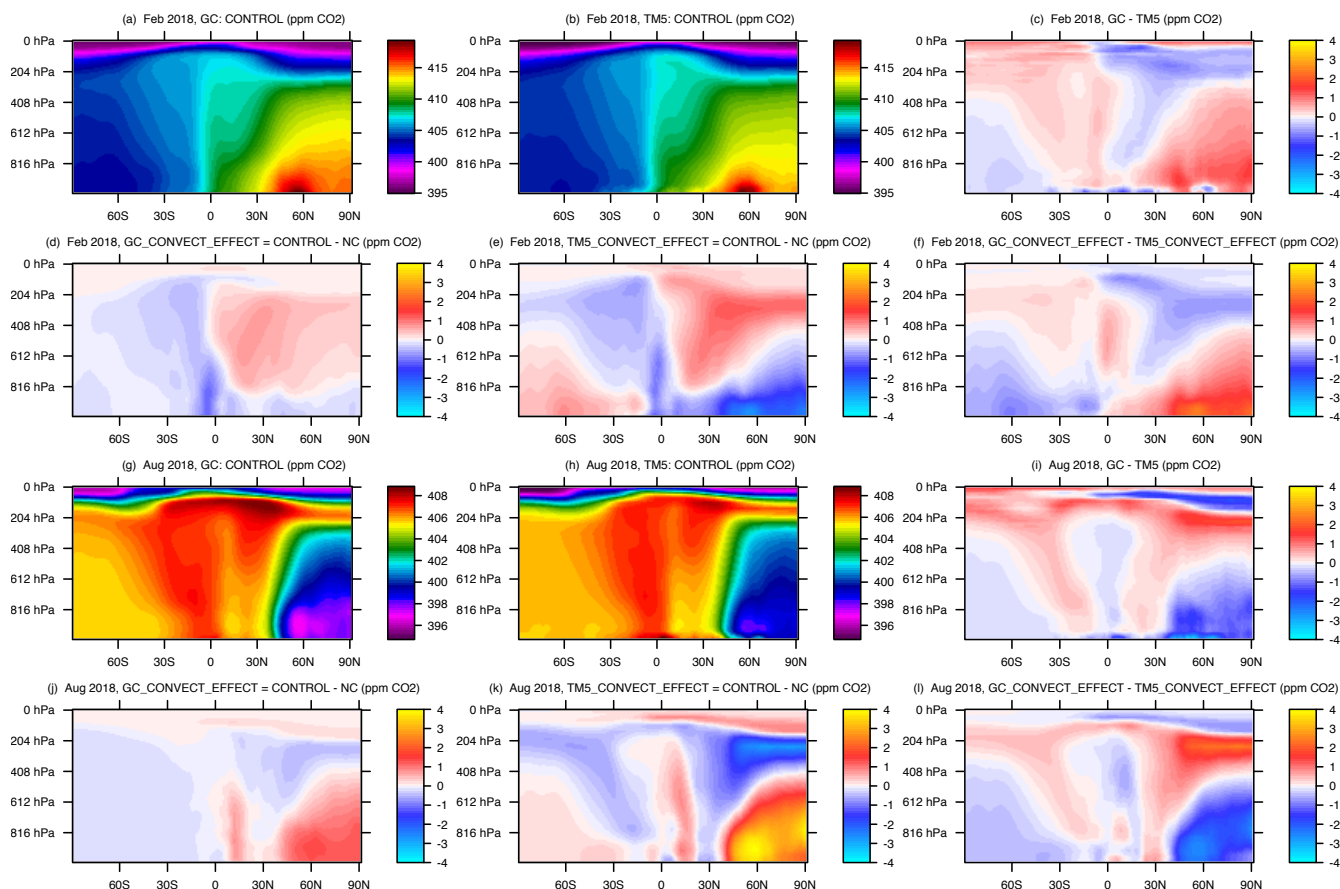
Figure 1. Vertical curtains of zonal-mean CO_2 dry-air mole fraction for February (top two rows) and August 2018 (bottom two rows). All quantities are monthly averages. The first and third rows (panels a-c and g-i respectively) show model control simulations and differences, averaged zonally. The second and fourth rows (panels d-f and j-l respectively) show the convective effect (control experiment minus the no convection, NC, experiment) in each model and the GEOS-Chem minus TM5 difference between them. The first column represents GEOS-Chem simulations, the second is TM5, and the third column is the GEOS-Chem minus TM5 difference.

The last two rows of Figure 1 show the same quantities as the first two, but for northern hemisphere summer (August). Terrestrial biosphere uptake results in a deficit of CO_2 in the troposphere poleward of the northern midlatitudes. Again the difference in convective effect (panel l) is visually similar to the control simulation differences (panel i).

3.2 XCO$_2$ differences

Zonal averages of the GEOS-Chem minus TM5 difference in XCO$_2$ as a function of latitude and time are shown in the middle two columns of Figure 2. Three-year averages of the differences are shown in side panels and present a possible proxy or metric for the transport error effect on annual source/sink estimates of CO_2 from inversions. As in the previous vertical curtain plots,
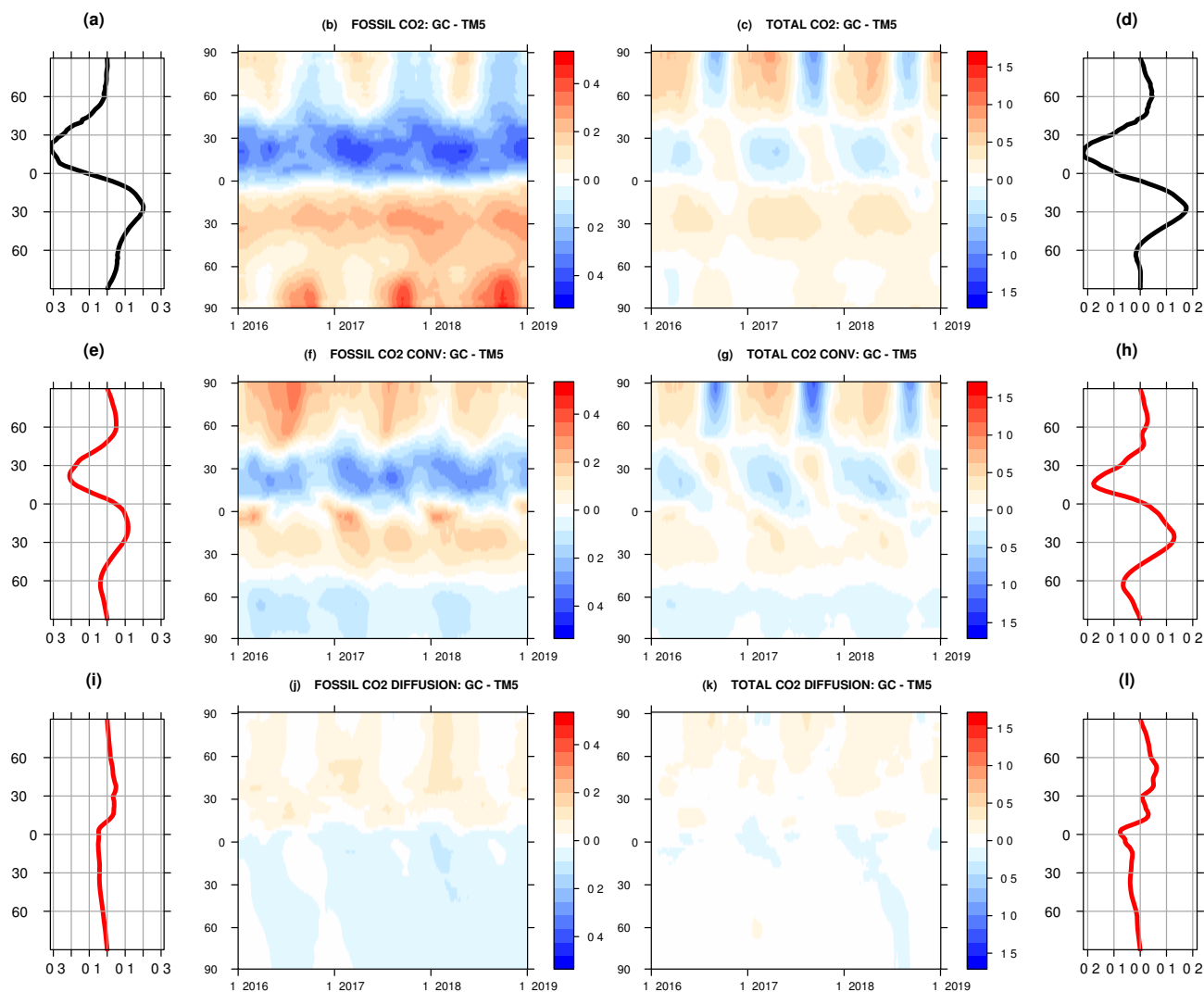
Figure 2. Zonally-averaged pressure-weighted average CO_2 differences between GEOS-Chem and TM5, plotted as function of latitude in side integrals and as a function of latitude and time in central panels, in dry-air mole fraction. Column 1 represents 3 year average of 2nd columns. Column 4 represents 3 year average of 3rd columns. Note the differences in scale between the fossil and total CO_2 plots.

195   the convective effect differences shown in the middle row of Figure 2 bear a strong resemblance to total difference between the control runs shown in the top row of Figure 2. Vertical diffusivity effects as a column average (bottom row of Figure 2) are of a much smaller magnitude. It is also worth pointing out that despite the strong seasonal patterns of differences seen in total CO_2 (panel c and g of Figure 2), the annual mean differences in total CO_2 (panel d and h of Figure 2) and fossil CO_2 (panel a and e of Figure 2) are quite similar and thus likely driven by differences arising from fossil fuels.
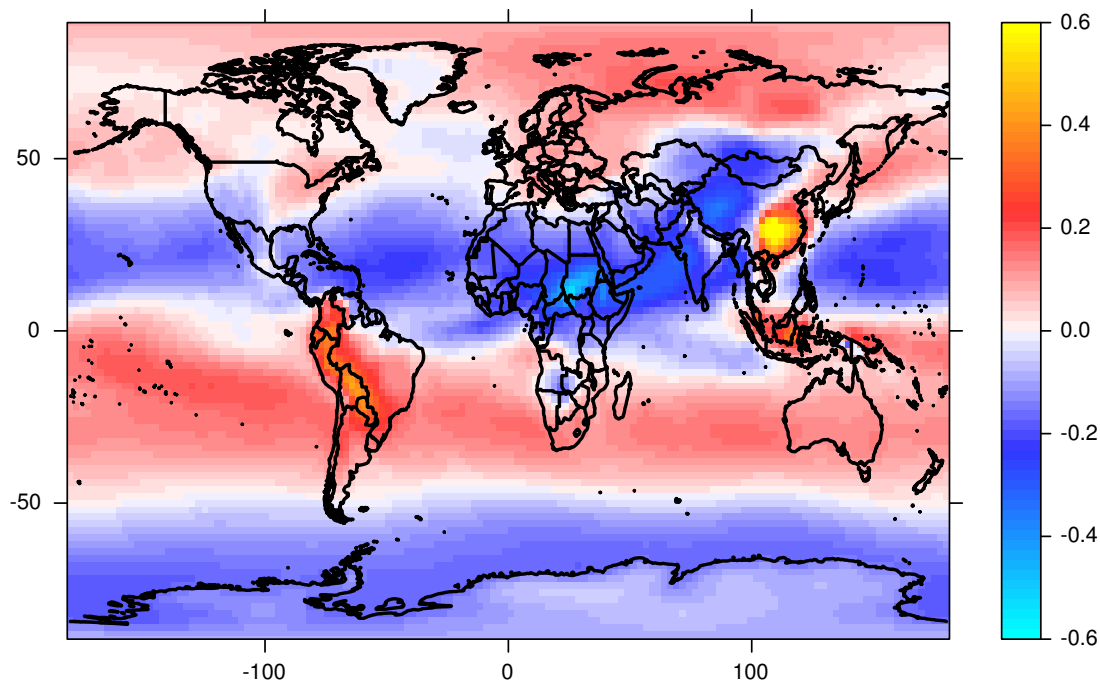
Figure 3. The 2016-2018 average XCO$_2$ difference between GEOS-Chem and TM5 "convective effects" (i.e. control - NC cases) using the TOTAL CO$_2$ tracer.

Figure 3 shows the 2016-2018 spatially-resolved time mean XCO$_2$ difference between GEOS-Chem and TM5. This figure illustrates the zonal variability of the XCO$_2$ differences, which was not shown in Figures 1 and 2. The large band of negative differences evidenced by the blue band in the lower northern latitudes is driven in large part by differences aloft, shown in Figure 1, and not from differences near the surface. There is an anomalously high difference over China, which is not due to a deviation of the difference pattern aloft but by a combination of weaker mixing in GEOS-Chem and anomalously strong fossil fuel emissions over Eastern China. Reproducing panel c of Figure 1 only over the area of enhancement in Figure 3, approximately 105°E to 120°E longitude results in PBL concentrations that are enhanced by 1-2 ppm CO$_2$ over the majority of the lower 20-25 % of the atmosphere and is the strongest contributor to the column average results in the spatial anomaly seen in Figure 3.

Seasonal summaries of the XCO$_2$ (Figure 2) subsetted into 45 degree latitude bands are shown in Figure S4. There is excellent agreement between the differences in convective effect and the differences in the control simulations, suggesting that convection differences between GEOS-Chem and TM5 are the predominant control on seasonal XCO$_2$ transport differences.
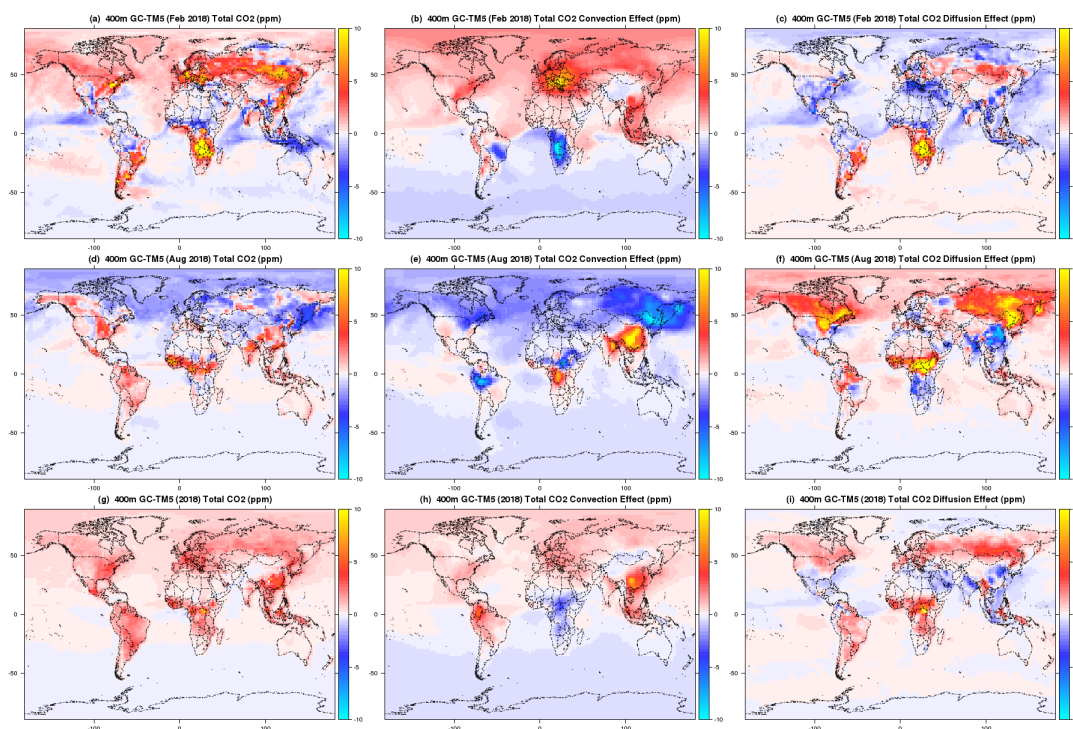
Figure 4. Monthly and annual average near surface model CO_2 differences. Results have been interpolated to the 2°x 2.5° GEOS-Chem grid and 400 meter height above ground level.

3.3   Impacts on near-surface CO_2

In the planetary boundary layer near intense surface sources and sinks of CO_2, the monthly average differences in diffusive effect between the models are on the order of 10 ppm (Figure 4). This is an order of magnitude larger than the model differences
215   in the column seen in Figure 2. There is a marked seasonality to the difference of CO_2 mole fraction at this level (leftmost column, panels a,d, and g), and the convective and diffusive effect patterns in both seasons (topmost two rows, panels a-f) appear anti-correlated at large scales. We will return to discuss this in Section 4

4   Discussion

Annual flux biases from convection uncertainty at zonal scales

220   Exploratory analysis on the location of long term carbon sinks is commonly performed by considering large zonal bands in order to contrast the tropics, extra-tropics and high latitudes (Stephens et al., 2007; Schimel et al., 2014), each of which has different mechanistic reasons to develop sources or sinks of carbon in a warming climate. The difference in convection effect

across CTMs, as seen in right hand column of Figure 2, generates a significant first-order bias on these important annual-zonal scales.

225 **Remaining model XCO$_2$ differences after accounting for convection**

An examination of panels (c) and panel (f) of Figure 1 shows that while the convective effect difference largely explains the control simulation differences between the two models away from the surface, it does not extend to the same altitude as the control simulation differences. This remaining difference bears some similarity to the difference in ND runs (Figures S2 and S3), indicating that while convection may be the main driver of the vertical differences in the model, it is likely that low level
230 PBL diffusivity differences also play a role.

Seasonal Cycle of XCO$_2$

Agreement on the seasonal cycle of XCO$_2$ appears quite good between the GEOS-Chem and TM5 control runs, with the amplitude of the average zonal seasonal differences on the order of 1 ppm or less at 45°N and poleward. GEOS-Chem minus TM5 differences in modeled seasonal cycles at TCCON locations are 10-15% of the amplitudes reported by Lindqvist et al.
235 (2015). While this difference is small, it is likely still significant to science hypotheses attempting to explain observed decadal scale changes in seasonal amplitude (Graven et al., 2013). Accounting for differences in convection reduces that difference by another order of magnitude, resulting in great agreement in XCO$_2$ on seasonal cycle amplitude. Hence a focus on improving the modeling of convective mixing of trace gases, particularly in CTMs, could have a significant impact on the ability to constrain high-latitude seasonality and inform ecological hypotheses.

240 **Regional Effects of Convection Uncertainty**

The effect of uncertainty in the parameterized modeling of vertical mixing, and convection in particular, drives systematic differences in XCO$_2$. These concentration differences then manifest themselves as the first order source of flux bias across large zonal bands amongst satellite CO$_2$ constrained flux inversion models (Schuh et al., 2019). However, in some regions there are notable exceptions to the zonal mean of transport differences. One of these is over eastern Asia in the general area of
245 China (Figure 3). This anomaly to the zonal average largely arises from model differences in the spatially-varying convection field (Taszarek et al., 2021) acting on large regional sources of CO$_2$ fossil fuel consumption (Schuh et al., 2022). While total CO$_2$ is plotted in Figure 3, one can see that the signal comes largely from the fossil fuel related portion of the CO$_2$ budget (cf. Figures S5, S6 and S7). Similar patterns emerge across areas of critical ecological and biological importance, such as the Amazon and equatorial Africa (Figure S7) and even emerge at the national scales there (Figure S8). These could result in
250 regional flux anomalies that are dependent on the particular CTM being used in a flux inversion.

Compensating effects of turbulent mixing and deep convection in PBL

While parameterized diffusion and convection cause mixing in different parts of the column, they both act to move signals of surface exchange up, away from the PBL and into the free troposphere. Historically, measurements of active and passive chemical species have been made more commonly within the PBL or at the surface than in the free troposphere. The availability
255 of measurements near the surface without a correspondingly strong constraint on upper atmospheric abundances means that those measurements speak strongly to the overall rate of ventilation of the PBL, and not necessarily which process is responsible for the needed mixing. We speculate that CTMs may meet this constraint using a different overall balance of convection and diffusion. The combination of remotely-sensed total column abundance with in situ measurements concentrated in the PBL may help to provide the needed constraint on vertical distribution to identify a correct balance of these mixing processes.

260 **Potential Issues with Direct Comparison of GEOS-Chem and TM5 convection implementations**

The parent models for GEOS-Chem and TM5 simulate convection differently. Some of the vertical movement associated with convection is explicitly resolved, depending on the model grid resolution. Non-resolved movement is parameterized using significantly different schemes. NASA's GEOS-5 MERRA2 reanalysis uses the Relaxed Arakawa-Schubert convection scheme (Moorthi and Suarez, 1992), an updraft-only detraining plume cloud model (Molod et al., 2012), to provide driving convective
265 mass fluxes used for GEOS-Chem. Version Cy31r2 of the Integrated Forecasting System (IFS) model was used to create the ERA-interim reanalysis (Dee et al., 2011) used to drive the present TM5 simulations. The IFS uses the Tiedtke convection scheme (Tiedtke, 1989), which provides upward and downward plume entrainment and detrainment mass fluxes at each model level. Both GEOS-Chem (Stanevich, 2018) and TM5 (Heimann and Korner, 2003) interpret convective mass fluxes from their parent models to drive relatively simple mixing schemes. This mixing can be represented by a matrix specifying exchange
270 among the layers in the column of a given grid cell.

While the RAS and Tiedtke convective parameterizations are different, we can still perform qualitative comparisons of the convective mass fluxes from the parent models under investigation here. The comparison (Figure S9) shows convective activity that is significantly different between the two models and highlights shallow convection features driving lower tropospheric mixing in TM5 that do not appear in GEOS-Chem. This would appear to support past research highlighting differences between
275 shallow convection features in MERRA and ERA-Interim (Posselt et al., 2012; Naud et al., 2014) This would suggest that the differences in CTM convective transport reported here result largely from differences in convection in the parent models as opposed to variations in how convective mixing is implemented in the CTMs. This confirms the findings of Folkins et al. (2006), Donner et al. (2007) and Orbe et al. (2017). Comparisons to long lived trace gases like SF_6 might allow more definitive conclusions about how differences in parent model convection, and differences in their re-implementations in CTMs, drive the
280 large-scale differences seen in this paper.

Looking forward

Recent analyses suggest that vertical transport in GEOS-Chem may be responsible for systematic biases in model performance against comparisons to CH_4 and SF_6 observations (Schuh et al., 2019; Stanevich et al., 2021). Part of this suspected vertical mixing issue may be due to imperfect reproduction of parent GEOS5 model transport (Yu et al., 2017). In preliminary analysis

285 of meridional gradients of trace gases, the GEOS5 parent model does not appear to exhibit the same systematic biases as the GEOS-Chem CTM (personal communication: Brad Weir, NASA-GMAO). When using offline parent convective mass flux fields, in theory, convective mixing of trace gases via resolved vertical velocity should be damped with increased averaging in time and space, and decreased horizontal model resolution (Yu et al., 2017). Furthermore, the coarse temporal nature, e.g. 3 hours or more, of the convective mass flux averaging leads to an information loss because the higher time resolution covariance

290 between tracer fields and vertical motion is lost. The resolved vertical velocity in 0.5° by 0.667° MERRA2 is similar in location and magnitude to that from the approximately 80km ERA-interim (personal communication: Sourish Basu, NASA-GMAO). This should not be surprising due to the similar horizontal resolutions of the model fields and suggests that the averaging of resolved vertical velocity fields to the coarser resolution CTM grids is likely not the reason for the differences shown in this paper.

295 A CTM's transport should asymptotically converge to the parent model's transport as model spatial and temporal resolution increases to the native resolution of the parent model, but this has not been demonstrated. Tests are currently under way with high time- and space-resolution GEOS5 meteorology via the GEOS-Chem High Performance (Martin et al., 2022) model to gauge this convergence. These tests will help to determine whether results such as Yu et al. (2017) are sufficient to explain all deficiencies in CTM vertical transport.

300 It is also worth noting that despite the clear patterns of difference in the large-scale convective mass fluxes from parent models used as inputs into GEOS-Chem and TM5 (see Figure S9), there are likely other factors at play which could cause differences in vertical transport. For its advection scheme, TM5 uses parent model mass fluxes and a corresponding flux form advection scheme, whereas GEOS-Chem explicitly uses interpolated parent model winds to diagnose mass fluxes for advection. The use of winds to drive advection, as opposed to mass fluxes, has been shown to be a likely source of errors and bias (Jöckel

305 et al., 2001). As a result of this, tests are also currently underway using the GEOS-Chem High Performance (Martin et al., 2022) model to investigate the magnitude of this bias and to what degree those model errors, and related errors in horizontal divergence, might be related to vertical transport in GEOS-Chem (personal communication, Sebastian Eastham).

5 Conclusions

The systematic large-scale patterns in XCO_2 differences associated with transport first presented in Schuh et al. (2019) have

310 been shown to result primarily from differences in the parameterization of convective mixing. This is the most important source of transport uncertainty for satellite-based flux inversion studies and of the same order as the expected biases in XCO_2 retrievals. Flux inversions using *in situ* measurements, which are more prevalent at the surface, should be much more sensitive to modeled vertical diffusion in the PBL than flux inversions using column average data.

The significance of uncertainty in simulated convection for model ensembles assimilating XCO_2, such as those of Crowell
315 et al. (2019) and Peiro et al. (2021), warrants further exploration of model convective parameterizations. Convection alone
drives 10-15% differences in XCO_2 seasonality between the two models studied here, and explains the vast majority of total
model differences in simulated XCO_2 seasonality. We also have shown that convection drives the majority of the meridional
difference in annual average XCO_2, a proxy for the meridional distribution of annual source and sinks in the related flux
inversion models. Therefore, we feel that future efforts to characterize transport uncertainty and how it relates to flux inversion
320 results would benefit tremendously from a more thorough exploration of differences in parent model convection.

Author contributions. Author contributions as follows: A. S. and A. J. wrote the manuscript. A. S. performed the GEOS-Chem CO_2 simula-
tions and performed analysis of results. A. J. was responsible for producing CT2017 and CT-NRT.v2019-2, and for running the perturbation
simulations with TM5.

Competing interests. None.

325 *Disclaimer.* None.

Acknowledgements. Funding for work came from NASA via funded proposals of A. S. and A. J. Specifically, OCO-2 Science Team project
(grant NNX15AG93G to Colorado State University and NNX12AP91G to the University of Colorado) and the Atmospheric Carbon and
Transport (ACT)-America project, a NASA Earth Venture Suborbital 2 project funded by NASA's Earth Science Division (NNX15AJ07G
to Colorado State University, and NNX15AJ06G to the University of Colorado). Results, analysis, and current publications related to the
330 underlying v9 MIP atmospheric inversion models are available at their website (https://www.esrl.noaa.gov/gmd/ccgg/OCO2_v9mip/)

References

Barnes, E. A., Parazoo, N., Orbe, C., and Denning, A. S.: Isentropic transport and the seasonal cycle amplitude of CO2, Journal of Geophysical Research: Atmospheres, 121, 8106–8124, https://doi.org/doi:10.1002/2016JD025109, 2016.

Bey, I., Jacob, D. J., Yantosca, R. M., Logan, J. A., Field, B. D., Fiore, A. M., Li, Q., Liu, H. Y., Mickley, L. J., and Schultz, M. G.: Global modeling of tropospheric chemistry with assimilated meteorology: Model description and evaluation, Journal of Geophysical Research: Atmospheres, 106, 23 073–23 095, https://doi.org/10.1029/2001JD000807, 2001.

Bosilovich, M. G.: Technical Report Series on Global Modeling and Data Assimilation, Volume 43 MERRA-2: Initial Evaluation of the Climate, Tech. rep., NASA-GMAO, https://gmao.gsfc.nasa.gov/pubs/docs/Bosilovich803.pdf, 2015.

Craine, J. M., Elmore, A. J., Wang, L., Aranibar, J., Bauters, M., Boeckx, P., Crowley, B. E., Dawes, M. A., Delzon, S., Fajardo, A., Fang, Y., Fujiyoshi, L., Gray, A., Guerrieri, R., Gundale, M. J., Hawke, D. J., Hietz, P., Jonard, M., Kearsley, E., Kenzo, T., Makarov, M., Marañón-Jiménez, S., McGlynn, T. P., McNeil, B. E., Mosher, S. G., Nelson, D. M., Peri, P. L., Roggy, J. C., Sanders-DeMott, R., Song, M., Szpak, P., Templer, P. H., der Colff, D. V., Werner, C., Xu, X., Yang, Y., Yu, G., and Zmudczyńska-Skarbek, K.: Isotopic evidence for oligotrophication of terrestrial ecosystems, 2, 1735–1744, https://doi.org/https://doi.org/10.1038/s41559-018-0694-0, 2018.

Crowell, S., Baker, D., Schuh, A., Basu, S., Jacobson, A. R., Chevallier, F., Liu, J., Deng, F., Feng, L., Chatterjee, A., Crisp, D., Eldering, A., Jones, D. B., McKain, K., Miller, J., Nassar, R., Oda, T., O'Dell, C., Palmer, P. I., Schimel, D., Stephens, B., and Sweeney, C.: The 2015-2016 Carbon Cycle As Seen from OCO-2 and the Global in situ Network, Atmospheric Chemistry and Physics Discussions, pp. 1–79, https://doi.org/https://doi.org/10.5194/acp-2019-87, 2019.

D'Arrigo, R., Jacoby, G. C., and Fung, I. Y.: Boreal forests and atmosphere–biosphere exchange of carbon dioxide, Nature, 329, 321–323, https://doi.org/doi:10.1038/329321a0, 1987.

Dee, D. P., Uppala, S. M., Simmons, A. J., Berrisford, P., Poli, P., Kobayashi, S., Andrae, U., Balmaseda, M. A., Balsamo, G., Bauer, P., Bechtold, P., Beljaars, A. C. M., van de Berg, L., Bidlot, J., Bormann, N., Delsol, C., Dragani, R., Fuentes, M., Geer, A. J., Haimberger, L., Healy, S. B., Hersbach, H., Hólm, E. V., Isaksen, L., Kållberg, P., Köhler, M., Matricardi, M., McNally, A. P., Monge-Sanz, B. M., Morcrette, J.-J., Park, B.-K., Peubey, C., de Rosnay, P., Tavolato, C., Thépaut, J.-N., and Vitart, F.: The ERA-Interim reanalysis: configuration and performance of the data assimilation system, Quarterly Journal of the Royal Meteorological Society, 137, 553–597, https://doi.org/https://doi.org/10.1002/qj.828, 2011.

Denning, A. S., Takahashi, T., and Friedlingstein, P.: Can a strong atmospheric CO2 rectifier effect by reconciled with a "reasonable" carbon budget?, Tellus, 51B, 249–253, 1999.

Dentener, F.: Interannual variability and trend of CH4lifetime as a measure for OH changes in the 1979–1993 time period, Journal of Geophysical Research, 108, https://doi.org/10.1029/2002JD002916, 2003.

Donner, L. J., Horowitz, L. W., Fiore, A. M., Seman, C. J., Blake, D. R., and Blake, N. J.: Transport of radon-222 and methyl iodide by deep convection in the GFDL Global Atmospheric Model AM2, Journal of Geophysical Research, 112, https://doi.org/doi:10.1029/2006JD007548, 2007.

Folkins, I., Bernath, P., Boone, C., Donner, L. J., Eldering, A., Lesins, G., Martin, R. V., Sinnhuber, B.-M., and Walker, K.: Testing convective parameterizations with tropical measurements of HNOsub3/sub , CO, Hsub2/sub O, and Osub3/sub : Implications for the water vapor budget, Journal of Geophysical Research: Atmospheres, 111, https://doi.org/https://doi.org/10.1029/2006JD007325, 2006.

Graven, H. D., Keeling, R. F., Piper, S. C., Patra, P. K., Stephens, B. B., Wofsy, S. C., Welp, L. R., Sweeney, C., Tans, P. P., Kelley, J. J., Daube, B. C., Kort, E. A., Santoni, G. W., and Bent, J. D.: Enhanced Seasonal Exchange of CO2 by Northern Ecosystems Since 1960, Science, 341, 1085–1089, https://doi.org/10.1126/science.1239207, 2013.

Gurney, K. R., Law, R. M., Denning, A. S., Rayner, P. J., Baker, D., Bousquet, P., Bruhwiler, L., Chen, Y.-H., Ciais, P., Fan, S., Fung, I. Y.,
370   Gloor, M., Heimann, M., Higuchi, K., John, J., Maki, T., Maksyutov, S., Masarie, K., Peylin, P., Prather, M., Pak, B., Randerson, J., Sarmiento, J. L., Taguchi, S., Takahashi, T., Tans, P., and Yuen, C.-W.: Towards robust regional estimates of CO_2 sources and sinks using atmospheric transport models, Nature, 415, 2002.

Heimann, M. and Korner, S.: The Global Atmospheric Tracer Model TM3 Model Description and User's Manual Release 3.8a, Tech. rep., Max-Planck-Gesellschaft, https://www.bgc-jena.mpg.de/bgc-systems/pmwiki2/uploads/Publications/5.pdf, 2003.

375   Holtslag, A. A. M. and Boville, B. A.: Local Versus Nonlocal Boundary-Layer Diffusion in a Global Climate Model, Journal of Climate, 6, 1825–1842, https://doi.org/10.1175/1520-0442(1993)006<1825:LVNBLD>2.0.CO;2, 1993.

Houweling, S., Dentener, F., and Lelieveld, J.: The impact of nonmethane hydrocarbon compounds on tropospheric photochemistry, Journal of Geophysical Research: Atmospheres, 103, 10 673–10 696, https://doi.org/10.1029/97JD03582, 1998.

Jöckel, P., von Kuhlmann, R., Lawrence, M. G., Steil, B., Brenninkmeijer, C. A. M., Crutzen, P. J., Rasch, P. J., and Eaton, B.: On a fundamen-
380   tal problem in implementing flux-form advection schemes for tracer transport in 3-dimensional general circulation and chemistry transport models, Quarterly Journal of the Royal Meteorological Society, 127, 1035–1052, https://doi.org/https://doi.org/10.1002/qj.49712757318, 2001.

Keeling, C., Bacastow, R., Carter, A., Piper, S., Whorf, T., Heimann, M., Mook, W., and Roeloffzen, H.: A three-dimensional model of atmospheric CO_2 transport based on observed winds: 1. Analysis of observational data, 1989a.

385   Keeling, C., Piper, S., and Heimann, M.: A three-dimensional model of atmospheric CO_2 transport based on observed winds: 4. Mean annual gradients and interannual variations, 1989b.

Krol, M., Houweling, S., Bregman, B., van den Broek, M., Segers, A., van Velthoven, P., Peters, W., Dentener, F., and Bergamaschi, P.: The two-way nested global chemistry-transport zoom model TM5: algorithm and applications, Atmospheric Chemistry and Physics, 5, 417–432, https://doi.org/https://doi.org/10.5194/acp-5-417-2005, 2005.

390   Lee, M. and Weidner, R.: JPL Publication 16-4: Surface Pressure Dependencies in the GEOS-Chem Adjoint System and the Impact of the GEOS-5 Surface Pressure on CO2 Model Forecast, Tech. rep., Jet Propulsion Laboratory California Institute of Technology Pasadena, California, 2016.

Lin, J.-T. and McElroy, M. B.: Impacts of boundary layer mixing on pollutant vertical profiles in the lower troposphere: Implications to satellite remote sensing, Atmospheric Environment, 44, 1726–1739, https://doi.org/https://doi.org/10.1016/J.ATMOSENV.2010.02.009,
395   2010.

Lin, S.-J. and Rood, R. B.: Multidimensional Flux-Form Semi-Lagrangian Transport Schemes, Monthly Weather Review, 124, 2046–2070, 1996.

Lindqvist, H., O'Dell, C. W., Basu, S., Boesch, H., Chevallier, F., Deutscher, N., Feng, L., Fisher, B., Hase, F., Inoue, M., Kivi, R., Morino, I., Palmer, P. I., Parker, R., Schneider, M., Sussmann, R., and Yoshida, Y.: Does GOSAT capture the true seasonal cycle of carbon dioxide?,
400   Atmospheric Chemistry and Physics, 15, 13 023–13 040, https://doi.org/doi:10.5194/acp-15-13023-2015, 2015.

Liu, J., Wennberg, P. O., Parazoo, N. C., Yin, Y., and Frankenberg, C.: Observational Constraints on the Response of High-Latitude Northern Forests to Warming, AGU Advances, 1, https://doi.org/https://doi.org/10.1029/2020AV000228, 2020.

Lloyd, J. and Farquhar, G. D.: Effects of rising temperatures and [CO 2] on the physiology of tropical forest trees, 363, 1811–1817, https://doi.org/10.1098/rstb.2007.0032, 2008.

405 Malhi, Y., BALDOCCHI, D. D., and JARVIS, P. G.: The carbon balance of tropical, temperate and boreal forests, 22, 715–740, https://doi.org/doi:10.1046/j.1365-3040.1999.00453.x, 1999.

Martin, R. V., Eastham, S. D., Bindle, L., Lundgren, E. W., Clune, T. L., Keller, C. A., Downs, W., Zhang, D., Lucchesi, R. A., Sulprizio, M. P., Yantosca, R. M., Li, Y., Estrada, L., Putman, W. M., Auer, B. M., Trayanov, A. L., Pawson, S., and Jacob, D. J.: Improved Advection, Resolution, Performance, and Community Access in the New Generation (Version 13) of the High Performance GEOS-Chem Global
410 Atmospheric Chemistry Model (GCHP), https://doi.org/https://doi.org/10.5194/gmd-2022-42, 2022.

Molod, A., Takas, L., Suarez, M., Bacmeister, J., Song, I., and Eichman, A.: The GEOS-5 Atmospheric General Circulation Model: Mean Climate and Development from MERRA to Fortuna, Tech. Rep. NASA/TM–2012-104606/Vol 28, National Aeronautics and Space Administration Goddard Space Flight Center, Greenbelt, Maryland, 2012.

Moorthi, S. and Suarez, M. J.: Relaxed Arakawa-Schubert. A Parameterization of Moist Convection for General Circulation Models, Monthly
415 Weather Review, 120, 978–1002, https://doi.org/10.1175/1520-0493(1992)120<0978:RASAPO>2.0.CO;2, 1992.

Naud, C. M., Booth, J. F., and Genio, A. D. D.: Evaluation of ERA-Interim and MERRA Cloudiness in the Southern Ocean, Journal of Climate, 27, 2109–2124, https://doi.org/https://doi.org/10.1175/JCLI-D-13-00432.1, 2014.

Norby, R. J. and Zak, D. R.: Ecological Lessons from Free-Air CO2 Enrichment (FACE) Experiments, 42, 181–203, https://doi.org/https://doi.org/10.1146/annurev-ecolsys-102209-144647, 2011.

420 Oda, T.: The Open-source Data Inventory for Anthropogenic CO_2 , version 2016 (ODIAC2016): a global monthly fossil fuel CO_2 gridded emissions data product for tracer transport simulations and surface flux inversions, Earth System Science Data, 10, 87–107, https://doi.org/https://doi.org/10.5194/essd-10-87-2018, 2018.

Orbe, C., Oman, L. D., Strahan, S. E., Waugh, D. W., Pawson, S., Takacs, L. L., and Molod, A. M.: Large-Scale Atmospheric Transport in GEOS Replay Simulations, Journal of Advances in Modeling Earth Systems, 9, 2545–2560,
425 https://doi.org/https://doi.org/10.1002/2017MS001053, 2017.

Peiro, H., Crowell, S., Schuh, A., Baker, D. F., O'Dell, C., Jacobson, A. R., Chevallier, F., Liu, J., Eldering, A., Crisp, D., Deng, F., Weir, B., Basu, S., Johnson, M. S., Philip, S., and Baker, I.: Four years of global carbon cycle observed from OCO-2 version 9 and in situ data, and comparison to OCO-2 v7, https://doi.org/http://doi.org/10.5194/acp-2021-373, 2021.

Penuelas, J., Fernández-Martínez, M., Vallicrosa, H., Maspons, J., Zuccarini, P., Carnicer, J., Sanders, T. G. M., Krüger, I., Obersteiner,
430 M., Janssens, I. A., Ciais, P., and Sardans, J.: Increasing atmospheric CO2 concentrations correlate with declining nutritional status of European forests, 3, https://doi.org/https://doi.org/10.1038/s42003-020-0839-y, 2020.

Peters, W., Jacobson, A. R., Sweeney, C., Andrews, A. E., Conway, T. J., Masarie, K., Miller, J. B., Bruhwiler, L. M. P., Petron, G., Hirsch, A. I., Worthy, D. E. J., van der Werf, G. R., Randerson, J. T., Wennberg, P. O., Krol, M. C., and Tans, P. P.: An atmospheric perspective on North American carbon dioxide exchange: CarbonTracker, Proceedings of the National Academy of Sciences of the United States of
435 America, 104, 18 925–18 930, https://doi.org/10.1072/pnas.07089861074, 2007.

Peylin, P., Law, R. M., Gurney, K. R., Chevallier, F., Jacobson, A. R., Maki, T., Niwa, Y., Patra, P. K., Peters, W., Rayner, P. J., Rödenbeck, C., van der Laan-Luijkx, I. T., and Zhang, X.: Global atmospheric carbon budget: results from an ensemble of atmospheric CO_2 inversions, Biogeosciences, 10, 6699–6720, https://doi.org/10.5194/bg-10-6699-2013, 2013.

Posselt, D. J., van den Heever, S., Stephens, G., and Igel, M. R.: Changes in the Interaction between Tropical Convection, Radiation, and the
440 Large-Scale Circulation in a Warming Environment, Journal of Climate, 25, 557–571, https://doi.org/doi:10.1175/2011JCLI4167.1, 2012.

Rienecker, M. M., Suarez, M. J., Gelaro, R., Todling, R., Bacmeister, J., Liu, E., Bosilovich, M. G., Schubert, S. D., Takacs, L., Kim, G.-K., Bloom, S., Chen, J., Collins, D., Conaty, A., da Silva, A., Gu, W., Joiner, J., Koster, R. D., Lucchesi, R., Molod, A., Owens, T., Pawson, S., Pegion, P., Redder, C. R., Reichle, R., Robertson, F. R., Ruddick, A. G., Sienkiewicz, M., and Woollen, J.: MERRA: NASA's Modern-Era Retrospective Analysis for Research and Applications, Journal of Climate, 24, 3624–3648, https://doi.org/https://doi.org/10.1175/JCLI-D-11-00015.1, 2011.

Schimel, D., Stephens, B. B., and Fisher, J. B.: Effect of increasing CO2 on the terrestrial carbon cycle, Proceedings of the National Academy of Sciences of the United States of America, 112, 436–441, https://doi.org/10.1073/pnas.1407302112, 2014.

Schuh, A. E., Jacobson, A. R., Basu, S., Weir, B., Baker, D., Bowman, K., Chevallier, F., Crowell, S., Davis, K. J., Deng, F., Denning, S., Feng, L., Jones, D., Liu, J., and Palmer, P. I.: Quantifying the Impact of Atmospheric Transport Uncertainty on CO_2 Surface Flux Estimates, Global Biogeochemical Cycles, 33, 484–500, https://doi.org/https://doi.org/10.1029/2018GB006086, 2019.

Schuh, A. E., Byrne, B., Jacobson, A. R., Crowell, S. M. R., Deng, F., Baker, D. F., Johnson, M. S., Philip, S., and Weir, B.: On the role of atmospheric model transport uncertainty in estimating the Chinese land carbon sink, Nature, 603, E13–E14, https://doi.org/https://doi.org/10.1038/s41586-021-04258-9, 2022.

Stanevich, I.: Variational data assimilation of satellite remote sensing observations for improving methane simulations in chemical transport models, Ph.D. thesis, https://tspace.library.utoronto.ca/handle/1807/89876, 2018.

Stanevich, I., Jones, D. B. A., Strong, K., Keller, M., Henze, D. K., Parker, R. J., Boesch, H., Wunch, D., Notholt, J., Petri, C., Warneke, T., Sussmann, R., Schneider, M., Hase, F., Kivi, R., Deutscher, N. M., Velazco, V. A., Walker, K. A., and Deng, F.: Characterizing model errors in chemical transport modeling of methane: using GOSAT XCH&ltsub&gt4&lt/sub&gt data with weak-constraint four-dimensional variational data assimilation, Atmospheric Chemistry and Physics, 21, 9545–9572, https://doi.org/https://doi.org/10.5194/acp-21-9545-2021, 2021.

Stephens, B. B., Gurney, K. R., Tans, P. P., Sweeney, C., Peters, W., Bruhwiler, L., Ciais, P., Ramonet, M., Bousquet, P., Nakazawa, T., Aoki, S., Machida, T., Inoue, G., Vinnichenko, N., Lloyd, J., Jordan, A., Heimann, M., Shibistova, O., Langenfelds, R. L., Steele, L. P., Francey, R. J., and Denning, A. S.: Weak northern and strong tropical land carbon uptake from vertical profiles of atmospheric CO_2, Science, 316, 1732–1735, 2007.

Taszarek, M., Allen, J. T., Marchio, M., and Brooks, H. E.: Global climatology and trends in convective environments from ERA5 and rawinsonde data, npj Climate and Atmospheric Science, 4, https://doi.org/https://doi.org/10.1038/s41612-021-00190-x, 2021.

Tiedtke, M.: A Comprehensive Mass Flux Scheme for Cumulus Parameterization in Large-Scale Models, Monthly Weather Review, 117, 1779–1800, 1989.

Wang, J., Feng, L., Palmer, P. I., Liu, Y., Fang, S., Bösch, H., O'Dell, C. W., Tang, X., Yang, D., Liu, L., and Xia, C.: Large Chinese land carbon sink estimated from atmospheric carbon dioxide data, Nature, 586, 720–723, https://doi.org/https://doi.org/10.1038/s41586-020-2849-9, 2020.

Wu, S., Mickley, L. J., Jacob, D. J., Logan, J. A., Yantosca, R. M., and Rind, D.: Why are there large differences between models in global budgets of tropospheric ozone?, Journal of Geophysical Research, 112, https://doi.org/doi:10.1029/2006JD007801, 2007.

Yu, K., Keller, C. A., Jacob, D. J., Molod, A. M., Eastham, S. D., and Long, M. S.: Errors and improvements in the use of archived meteorological data for chemical transport modeling, Geoscientific Model Development Discussions, pp. 1–22, https://doi.org/https://doi.org/10.5194/gmd-2017-125, 2017.